Nitrogen processing by treatment wetlands in a tropical catchment dominated by agricultural landuse.

Author

Kavehei, E, Roberts, ME, Cadier, C, Griffiths, M, Argent, S, Hamilton, DP, Lu, J, Bayley, M, Adame, MF

Published

2021

Journal Title

Marine Pollution Bulletin

Version

Accepted Manuscript (AM)

DOI

10.1016/j.marpolbul.2021.112800

Nitrogen processing by treatment wetlands in a tropical catchment dominated by agricultural landuse

E Kavehei[a], M. E. Roberts[a], C. Cadier[a], M. Griffiths[b], S. Argent[c], D. Hamilton[a], J. Lu[a], M. Bayley[d], M. F. Adame[a]*

[a] Australian Rivers Institute, Griffith University, Nathan, 4111, QLD, Australia

[b] Department of the Environment and Science, Queensland Government, Brisbane, QLD, 4000, Australia

[c] Terrain Natural Resource Management, Cairns, 4870, QLD, Australia

[d] Australian Wetlands Consulting Pty Ltd, Bangalow, 2479, NSW, Australia

*corresponding author: f.adame@griffith.edu.au

Abstract

Agriculture is a major contributor to marine nitrogen pollution, and treatment wetlands can be a strategy to reduce them. However, few studies have assessed the potential of these systems in tropical regions. We quantify the nitrogen removal rates of four recently constructed treatment wetlands in tropical Australia. We measured denitrification potential (D_t), the inflow-outflow of nutrients, and tested whether the environment in these tropical catchments is favourable for nitrogen removal. D_t was detected in three of the four systems with rates between 2.0 to 12.0 mg m^2 h^{-1}; the highest rates were measured in anoxic soils (-100 to 300 mV) that were rich in carbon and nitrogen (> 2% and > 0.2%, respectively). The highest nitrogen removal rates were measured when NO_3^--N concentrations were > 0.4 mg L^{-1} and when water flows were slow. Treatment wetlands in tropical regions can deliver the removal of nitrogen and other pollutants attached to sediment from the receiving water to reduce its impacts on sensitive coastal zones such as the Great Barrier Reef.

Keywords: constructed wetlands; Great Barrier Reef, nitrate; sugarcane; water quality

1. Introduction

Nitrogen pollution is an environmental problem that affects receiving waters of most agricultural regions of the world. Fertiliser runoff is a significant source of surface and groundwater nitrogen pollution (Almasri and Kaluarachchi, 2004; Wang et al., 2015). About half of the reactive nitrogen from agricultural fertilisers is used by target crops, but the rest will end up in downstream receiving environments, causing ecosystem degradation (Galloway and Cowling, 2002; Galloway et al., 2003). Agricultural "best management practices" are an essential first step to address the problem, but the construction of treatment systems can complement these efforts. These include "treatment wetlands", which are structures designed to simulate the ecological processes of natural wetlands (Land et al., 2016). Treatment wetlands can improve water quality through biological processes involving vegetation, soils, and microbial communities that remove N from land runoff, but also phosphorus and total suspended solids (TSS) (Rousseau et al., 2008; Land et al., 2016; Haritash et al., 2017). In some regions, treatment wetlands can be as efficient at reducing nitrogen loads as land management strategies (Hansen et al., 2018). Thus, significant investments globally have been directed in treatment wetlands for improving water quality in urban and agricultural landscapes (Jones et al., 2012).

Wetlands are recognised for their provision of valuable ecosystem services, including water quality improvement (Mitsch and Gosselink, 2000); however, few studies have assessed the benefits of treatment wetlands in tropical regions. The performance of treatment wetlands is likely to be different in temperate than tropical climates, where temperatures and productivity are high year-round, and rainfall and flooding can be intense and frequent. In the Great Barrier Reef catchments, rainfall runoff events can carry high loads of nutrients into coastal waters (Davis et al., 2017). These conditions create denitrification "hot-times" and "hot-spots" where nitrogen amelioration is likely to be high (Adame et al., 2019b).

This study examined whether the conditions found in tropical agricultural landscapes (high temperature, high productivity, high runoff of nitrate-nitrogen (NO_3^--N)) are favourable for nitrogen removal. We measured the denitrification potential of four treatment systems, changes in nutrient concentrations from the inlet-outlet, and analysed environmental factors associated with nutrient removal. Also, we used a mathematical model that includes the effect of water flows and vegetation on the transformations of nitrogen to investigate the optimal conditions for these treatment wetlands to remove pollutants and protect adjacent marine ecosystems.

2. Methods

2.1 Study sites

This study was conducted in the Tully and Johnstone catchments, both within the Great Barrier Reef region of Australia (Fig.1). The wetland treatment sites have wet tropical climates with an annual mean rainfall of 4,075 mm and annual mean minimum and maximum temperatures of 19.3 and 28.2 °C, respectively. The region has two defined seasons, a dry and cool (June to November; 168 - 200 mm monthly rainfall and mean a minimum of 15.2 °C and mean maximum of 23.9 °C) and a hot and wet season (December to May, 267 - 756 mm and 20.6 to 31.2°C; Tully Sugar Mill Station, 32042; 1925- 2020, and South Johnstone Exp. Station, 032037; 1944- 2020; Australian Bureau of Meteorology, 2020).

The four treatment wetlands were constructed between late 2018 and mid-2019 as part of a government initiative (Major Integrated Projects, Queensland Government) to reduce nitrogen loads into waterways that discharge into the Great Barrier Reef. However, TW1 was constructed later in November 2019. Three of the wetland treatment systems (TW1, TW2, TW3) are considered “embellished wetlands”, which refers to the modification of small

drains or features of the landscape (< 2 ha) to reconfigure their hydrology and create conditions similar to natural wetlands. The fourth system is considered a "landscape wetland" (TW4) as it is a large project (> 8 ha) that required major earthworks. The sites are within agricultural areas, predominantly sugarcane and banana plantations (Table 1).

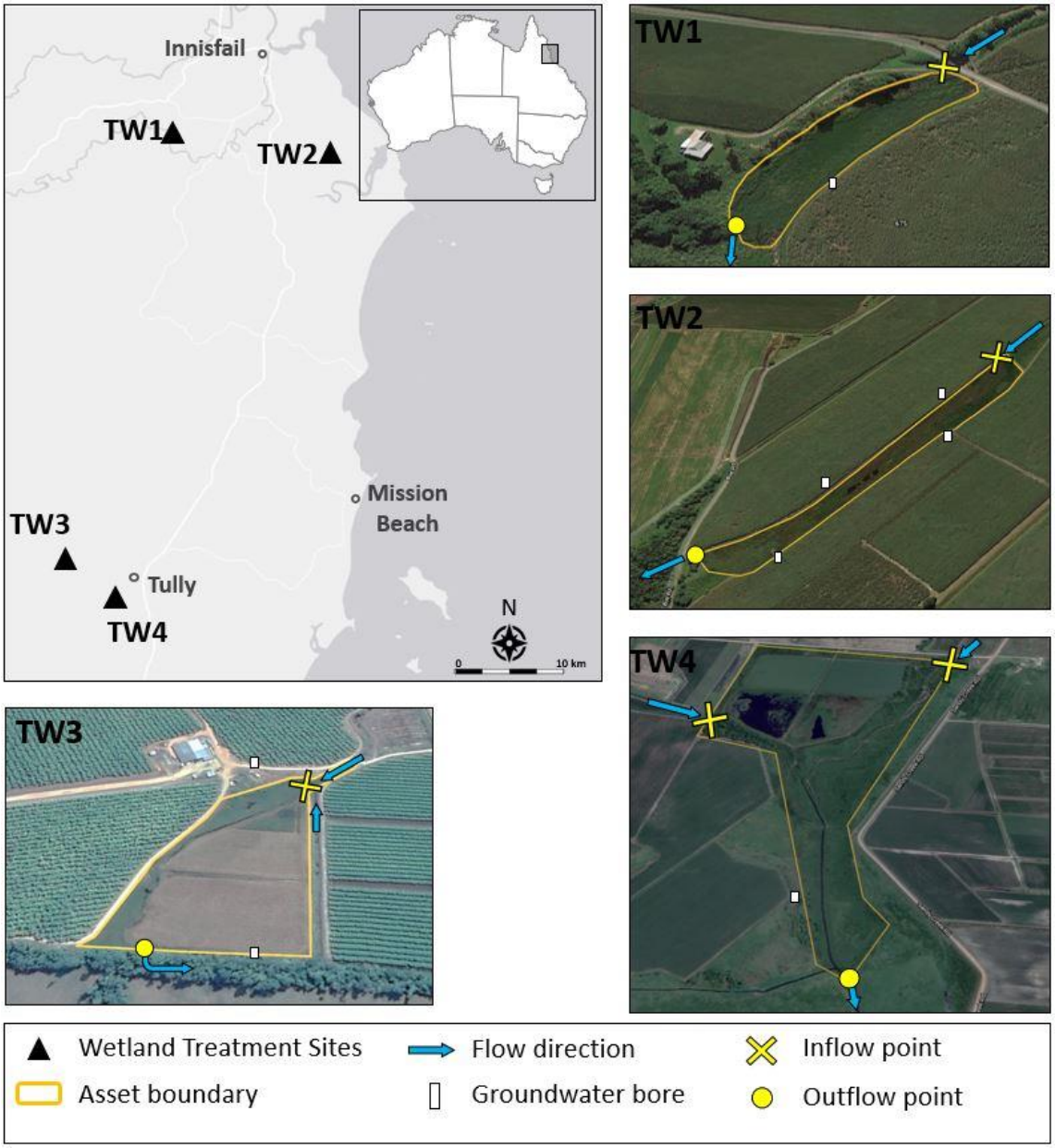

Figure 1. Map of Australia, location of the sites, and the sampling points within each site.

Table 1. Description of study sites, area (ha), land use for their catchment, and wetland to catchment area ratio.

Site	Catchment	Wetland area (ha)	Targeted land use area (ha)	Wetland: catchment	Targeted land use
TW1	Johnston	0.3	18	0.02	Sugarcane
TW2	Moresby	1.6	15	0.11	Sugarcane
TW3	Tully	1.2	37	0.03	Banana
TW4	Tully	8.5	368	0.02	Sugarcane

91

92 **2.2 Environmental characteristics**

93 During the dry season of 2019, surface soil samples (top 10 cm) were collected at each site in
94 triplicates. The soil was collected with a plastic 50 mL mini core. The volume and weight of
95 each sample were recorded, and the samples were oven-dried at 60 ˚C for at least 48 h. The
96 dry weight of each sample was used to measure bulk density (g cm^{-3}). Subsamples of the
97 dried soil were ground and analysed for nitrogen and organic carbon (C%) with an elemental
98 analyser (EA-IRMS, Serco System, Griffith University). Additional soil samples were
99 analysed for grain size by sieving a composited sample of sediment taken from five replicates
100 within each site. The soil was mixed, and a representative 500 g sample was wet-sieved
101 through five mesh sizes: 38, 150, 250, 500, and 4,000 µm. Water temperature, electrical
102 conductivity (EC), and pH were measured at each site at five locations randomly selected
103 with a calibrated water quality meter (ProPlus, YSI meter, OH, USA). Oxidation-reduction
104 potential (ORP) was also measured with a redox meter (HQ11d, Hach Pacific, Australia) at
105 five locations at the sediment-water interface.

106

107

108

2.3 Denitrification

In December 2019, areal rates of denitrification by the bottom sediments were estimated for each site with the isotope pairing technique (Nielsen, 1992) adapted to wetlands (Adame et al., 2019a). Briefly, the method consists of adding enriched ^{15}N-nitrate at a saturating concentration to overlying water and estimating denitrification rates from $^{15}N\text{-}N_2$ gas production. This technique has three main assumptions: (1) $^{15}NO_3^-$ addition does not significantly increase denitrification outside its natural range, (2) $^{15}NO_3^-$ added and $^{14}NO_3^-$ in the sediment are uniformly mixed, and (3) a stable gradient of $^{15}NO_3^-$ across the sediment-water interface is rapidly established during the experiment relative to the incubation time (Nielsen, 1992; Steingruber et al., 2001; Robertson et al., 2019). To ensure these assumptions were met, we maintained well-mixed conditions in the overlying water over short incubation (5 h) periods with NO_3^--N concentrations similar to those naturally found at the sites.

The experiments were conducted with eight intact sediment cores (8 cm depth) per site, which were sampled with Perspex tubes (4.8 cm internal diameter × 30 cm long). The cores were capped at the bottom and filled with water from the site and left to equilibrate overnight. The following day, the cores from each site were placed standing in a rack within a large container filled with water to maintain a constant temperature throughout the experiment. The temperature of the surrounding water in the container was maintained between 28 and 32 °C throughout the experiment. The $^{15}N\text{-}NO_3^-$ was added to each core at the beginning of the experiment, topped with water, and sealed to maintain low oxygen conditions. A Teflon-coated stirrer bar was connected to the lid of each container, suspended 5 cm above the sediment, and stirred by an external rotating magnet to homogenise the water in the container. Three replicates of water samples were obtained before and after enrichment with $^{15}N\text{-}NO_3^-$, to measure NO_3^- enrichment during the experiment (ε). The replicates were filtered through a 0.45 µm membrane filter, stored in 25 mL tubes, and frozen before being

analysed for ammonium-nitrogen (NH_4^+-N) and oxidised nitrogen (NO_x^--N = NO_3^- + NO_2^-) (colourimetric analyses based on APHA/AWWA/WPCF, 2012; Chemistry Centre, Queensland Department of Environment and Science, Brisbane, Australia). Detection limits (mg L^{-1}) were: 0.002 for NH_4^+-N and 0.001 for oxidised nitrogen.

After 20 minutes of incubation, two cores were sacrificed by adding 1 ml of 50% of zinc chloride ($ZnCl_2$). The slurry was thoroughly mixed, and three replicates of 10 mL were taken from each core in Exetainer vials (Labco, High Wycombe, UK) with 250 µL of 50% w/v $ZnCl_2$. The same procedure was repeated for three cores at two hours, and for another three cores at five hours to estimate changes in ^{15}N-NO_3 concentration. The gas within each vial was analysed by continuous-flow mass spectrometry for $^{28}N_2$, $^{29}N_2$, and $^{30}N_2$-gas (EA-IRMS, Serco System at Griffith University). Denitrification rates are reported as nitrogen loss in mg m^{-2} h^{-1} for ambient light conditions, with a detection limit of 0.01 mg m^{-2} h^{-1}, calculated from equations in Steingruber et al. (2001).

D_{15} is denitrification rate of labelled $^{15}NO_3^-$ from production rate of $^{29}N_2$ and $^{30}N_2$:

$$D_{15} = r_{29} \times 2(r_{30}) \quad (1)$$

Where r_{29} and r_{30} are the production rates of $^{29}N_2$ and $^{30}N_2$, respectively.

D_{14} is denitrification rate of unlabelled $^{14}NO_3$:

$$D_{14} = D_{15} \times \frac{r_{29}}{2(r_{30})} \quad (2)$$

and D_t is total denitrification rate:

$$D_t = D_{15} + D_{14}. \quad (3)$$

D_w^{tot} is total denitrification rate of NO_3^- in the water column:

$$D_w{}^{tot} = \frac{D_{15}}{\varepsilon} \quad (4)$$

where ε is NO_3^- enrichment during incubation as a result of $^{15}NO_3^-$ additions:

$$\varepsilon = \left(\frac{[NO_3{}^-]_a - [NO_3{}^-]_b}{[NO_3{}^-]_a}\right)$$

Where *a* and *b* refer to concentrations after and before $^{15}NO_3^-$ addition.

D_w is denitrification rate in the water column corrected for tracer addition:

$$D_w = D_w{}^{tot}(1 - \varepsilon). \quad (5)$$

and D_n is coupled nitrification-denitrification:

$$D_n = D_t - D_w{}^{tot} \quad (6)$$

2.4 Inflow, outflow sample collection, and analysis

The sampling design for each site was different, but at least one inflow and one outflow point was measured for at least one wet season per site (Fig. 1). Additionally, groundwater samples about one meter depth were obtained from piezometers installed at each of the sites. The sites TW1, TW2, and TW4, were sampled 11 to 12 times between December 2019 and June 2020, and TW3 was sampled 27 times from February 2019 to June 2020. Daily precipitation was obtained from local weather stations (TW1: Central Mill Alert, Bureau No.: 032160; TW2: Cowley Beach, Bureau No.:032194; TW3 and TW4: Tully Sugar Mill, Bureau No.: 032042). Water level data were monitored for TW3 and TW4 sites using electronic water level loggers (HOBO® U20L-04).

Surface water samples were analysed for pH, ORP, dissolved oxygen (DO), EC, turbidity (NTU), nitrogen (total nitrogen (TN), total ammoniacal-nitrogen (NH_3-N + NH_4^+-N), NO_x^--N, nitrite (NO_2)), phosphorus (total phosphorus (TP), Organophosphorus (OP)) and

TSS. From these nutrient concentrations, we calculated nitrate ($NO_3 = NO_x - NO_2$), dissolved inorganic nitrogen (DIN = NH_4^+-N + NO_x^--N), and dissolved organic nitrogen (DON = TN – DIN). Nitrite was below detection limits in most samples. Most ammoniacal nitrogen is in the form of NH_4^+-N at pH < 8; thus, we considered that NH_3-N concentrations were negligible. Throughout the report, concentrations are shown as mean ± standard error (mg L^{-1}). The removal and release of nutrients in the wetlands are shown as changes in concentration: inflow concentration – outflow concentration. For TW2, which is highly influenced by groundwater, inflow nutrient concentrations were considered an average of surface inflows and the groundwater obtained from the piezometers.

2.5 Statistical analysis

To test whether differences between inflow and outflow constituent concentrations were significantly different from zero, we used a one-sample, one or two-tailed t-test for each nutrient and TSS per site. Differences in physicochemical parameters (DO, pH, ORP, conductivity, and turbidity) between inflow and outflow were tested with a paired two-sample t-test. A bivariate correlation was used to determine the relationship between removal and inflow concentrations. To assess the influence of physicochemical parameters and removal rates, we conducted a stepwise multiple regression after checking for autocollinearity among parameters. A scatterplot of the residuals was checked for homoscedasticity in the regression. Normality and homogeneity of variance were tested using residual plot analyses, Shapiro-Wilk and Kolmogorov-Smirnov tests. When a parameter distribution was not normal, it was transformed (log_{10}). If normality was not achieved, even with transformation, a non-parametric test (one-sample Wilcoxon signed-rank test or independent-samples Mann-Whitney U Test) was conducted. The significance level was set at 0.05. Statistical analyses were performed with SPSS (v24, IBM, New York, USA).

2.6 Modelling performance of constructed wetlands

A mathematical model for nitrogen transformations within the wetlands was used to model the performance of wetlands TW3 and TW4, where hydrological data were available. Two cases were considered, a steady-state system with constant inflows and an event-based case. The mathematical model (see Eqns 8 – 13 of Adame et al. (2019b)) consists of a series of ordinary differential equations that describe the processes that may result in the uptake of different forms of N, NO_3^--N or NH_4^+-N, and affect concentrations of DON, particulate nitrogen (PN), and TN. The model used the following parameters:

Denitrification rate: reduction of NO_3^- to nitrite (NO_2^-), NO, N_2O, and finally to N_2. The inputs for the models were the rates measured in this study.

Nitrification rate: oxidation of NH_4^+-N to NO_2^- followed by oxidation to NO_3^-.

Plant uptake: uptake by macrophytes of NH_4^+-N and NO_3^-. The uptake was estimated from the growth rates of macrophytes in tropical Australia (Adame et al., 2017) and a stoichiometric conversion factor for C:N of 50.

Anammox rate: anaerobic ammonium oxidation, or the conversion of NH_4^+-N and NO_2^- to gaseous N_2.

Sedimentation rate: accumulation in wetland sediments of PN, associated with nitrogen from particulate organics and TSS.

Mineralisation rate: decomposition of organic matter, producing NH_4^+-N and DON.

Ammonification rate: Microbial conversion of DON to NH_4^+-N.

A summary of the rate constants and half-saturation constants for the nitrogen processes is shown in Supplementary Data (Table S1).

Wetlands TW3 and TW4 were modelled using the steady-state and event-based model. For the steady-state model, we assumed a constant flux of water through the system, with the wetland volume held constant and rainfall and evaporation effects not included. For TW3, we considered a vegetated and non-vegetated scenario. In the non-vegetated scenario, plant uptake and denitrification were set to zero in the model. We considered three different nutrient concentrations (low, medium, and high) for NH_4^+-N, NO_3^-, DON, particulate organic nitrogen (PON), and TSS, across ten different inflow rates with a total of 30 scenarios for each wetland. The constituent concentrations for the low, medium and high scenarios are shown in Supplementary Data (Table S2)

For the event-based model, we used inputs of nutrient concentrations in the inflow, rainfall, water elevation, and temperature. The inflow and wetland surface area and volume were calculated based on the water elevation and theoretical relationships among elevation, inflow, surface area, and volume, as used for the steady-state analysis. Models of constituent inflow concentrations were developed using a multiple linear regression between the observed concentrations at the inflow location, rainfall, 3-day antecedent rainfall, and the water elevation. As no PON observations were available, a constant concentration of 1.69 mg L^{-1} was used for the models.

The event-based model was used to simulate nitrogen processes in TW3 for 121 days, commencing on 4 February 2020. Eleven observations were available during this period. All available data were used in training (no independent test dataset) to simulate inflow concentrations, obtaining coefficient of determination (R^2) values of 0.52 and 0.53 for NH_4^+-N and NO_3^--N, respectively. The DON concentrations were unable to be related to rainfall and water elevation; thus, we used the median observed DON concentration of 0.19 mg L^{-1}.

3. Results

3.1 Environmental characteristics

The soil was dominated by clay and silt (< 38 µm) in all sites, with contributions reaching > 90% in TW1 and TW3. Site TW2 had the highest contribution of sand (150-500 µm), with 14.2 %, while TW4 had the highest contribution of gravel (> 4,000 µm), with 9.1% (Table 2). The soil carbon content ranged from 1.7 – 9.0%, with the lowest and highest values measured in TW3 and TW4, respectively. Sites TW1 and TW4 also had the highest values for soil nitrogen content of 0.31%. The C:N (molar ratio) ranged from 11 to 17 in all sites except TW4, which had much higher values at 34 (Table 2). TW1 and TW4 had the lowest and highest average NO_3^--N concentrations in the inflow water with 0.06 ± 0.02 mg L^{-1} and 0.28 ± 0.05 mg L^{-1}, respectively (Table 2). Among all sites, TW2 had the highest DON concentrations at 0.55 mg L^{-1}.

Table 2. Soil characteristics, grain size composition, and average inflow water characteristics of the treatment wetlands in the Wet Tropics.

Parameters	TW1	TW2	TW3	TW4
Soil characteristics				
%C of dry wt	3.9 ± 1.2	2.0 ± 0.32	1.7 ± 0.27	9.0 ± 0.76
%N of dry wt	0.31 ± 0.09	0.13 ± 0.02	0.18 ± 0.03	0.31 ± 0.03
C:N (molar ratio)	14 ± 0.89	17 ± 0.45	11 ± 0.07	34 ± 5.2
ORP (mV)	325 ± 38	256 ± 17	-99 ± 11	300 ± 70
Bulk density (g cm^{-3})	0.68 ± 0.11	1.2 ± 0.08	0.81 ± 0.07	0.99 ± 0.12
Grain size < 38µm (%)	89.8	66.0	95.6	71.4
Average of inflow surface water characteristics				
Temperature (°C)	25.0 ± 1.2	28.5 ± 1.2	25.4 ± 0.6	27 ± 0.5
EC (µS cm^{-1})	114 ± 21	301 ± 221	112 ± 4	73 ± 12

pH	6.1± 0.1	5.5 ± 0.3	6 ± 0.1	5.8 ± 0.1
DO (%)	52 ± 13	115 ± 17	52 ± 8	84 ± 5
NO_3^--N (mg L^{-1})	0.06 ± 0.02	0.15 ± 0.13	0.12 ± 0.03	0.28 ± 0.05
NH_4^+−N (mg L^{-1})	0.04 ± 0.01	0.02 ± 0.01	0.05 ± 0.01	0.03 ± 0.00
DON (mg L^{-1})	0.45 ± 0.07	0.55 ± 0.05	0.23 ± 0.02	0.18 ± 0.02
OP (mg L^{-1})	0.07 ± 0.02	< 0.01	0.02 ± 0.00	0.03 ± 0.00
TP (mg L^{-1})	0.32 ± 0.03	0.03 ± 0.01	0.14 ± 0.02	0.07 ± 0.01

Note: ORP: oxidation-reduction potential; EC: electrical conductivity; DO: dissolved oxygen; NO_3^--N: nitrate-nitrogen; NH_4^+−N: ammonium-nitrogen; DON: dissolved organic nitrogen; OP: organophosphorus; TP: total phosphorus.

256

257 **3.2 Denitrification**

258 During the denitrification experiments, the pH of the water ranged from 4.8 in TW2 to 5.8 in
259 TW1. The ORP of the water was oxic with values > 250 mV in all sites, except in TW3,
260 where values were close to -100 mV (Table 3). The total denitrification potential as nitrogen
261 removal of the sites ranged from non-detectable in TW1 to 12.0 mg m^{-2} h^{-1} in TW3 (Table 3).
262 From the denitrification measured, most of it was fuelled from NO_3^--N in the water column
263 (D_w^{tot}) in TW3 and TW4. By contrast, in TW2, most denitrification (> 75%) was coupled
264 with soil nitrification (D_n). The nutrient analyses from the overlying water showed that NO_3^--
265 N concentrations were highest (3.49 ± 2.1 mg L^{-1}) in the TW2 soil cores. The TW3 cores
266 showed the lowest NO_3^--N but the highest NH_4^+-N concentrations of 0.004 ± .001 and 0.85 ±
267 1.8 mg L^{-1}, respectively.

268

269

270

271

Table 3. Denitrification rates (mean ± standard error; mg m^{-2} h^{-1}) of the treatment wetlands and the experimental background conditions of ORP, NO_3^--N, and NH_4^+-N.

Sites	TW1	TW2	TW3	TW4
D_t	n.d	2.2 ± 3.1	12.0 ± 3.0	6.3 ± 2.8
D_w^{tot}	n.d	0.58 ± 0.83	11.1 ± 2.7	6.0 ± 2.6
D_n	n.d	1.6 ± 2.3	0.91 ± 0.22	0.29 ± 0.13
D_w	n.d	0.43 ± 0.61	0.84 ± 0.21	0.28 ± 0.12
ε	0.10	0.26	0.92	0.95
Experiment background conditions				
ORP (mV)	325 ± 38	256 ± 17	-99 ± 11	300 ± 70
NO_3^- −N (mg L^{-1})	0.34 ± 0.1	3.49 ± 2.14	0.004 ± 0.001	0.002 ± 0.000
NH_4^+−N (mg L^{-1})	0.25 ± 0.18	0.54 ± 0.5	0.85 ± 0.18	0.014 ± 0.001

Note: Dt = total denitrification; D_w^{tot} = denitrification of nitrate from the water column; D_n = coupled nitrification-denitrification; D_w = denitrification corrected for nutrient additions during experiments; ε = NO_3^--N enrichment.

3.3 Inflow versus outflow water

The physicochemical characteristics of the water changed as it flowed through the treatment systems. The pH increased in the outflow of TW2 and TW4 compared to their inflow (U = 55, Z = *-1.90*, $p \geq 0.05$; t (50) = -3.45, $p < 0.01$), while DO decreased in the outflow, probably as a result of respiration (t (26) = *2.53*, $p < 0.05$; t (50) = *7.39*, $p < 0.001$, Fig. 2). In contrast, the outflow from TW1 showed a significant decrease in pH (t (11.58) = 4.01, $p <$ 0.01) and a significant increase in DO level (t (18) = -3.64, $p < 0.01$) compared to its inflow. The pH and DO did not significantly differ between inflow and outflow of TW3 ($p > 0.6$), and remained at around 6 and 50%, respectively. The EC significantly decreased in the outflow of TW3 (t (48) = 2.54, p = < 0.05); however, for TW4, EC increased in the outflow compared to its inflow (t (35.29) = -2.25, $p < 0.05$). In all sites, the turbidity of water was

286 lower in the outflow than the inflow, however, the difference was only significant in TW1 (t

287 (18) = 5.06, $p < 0.001$) (Fig. 2)

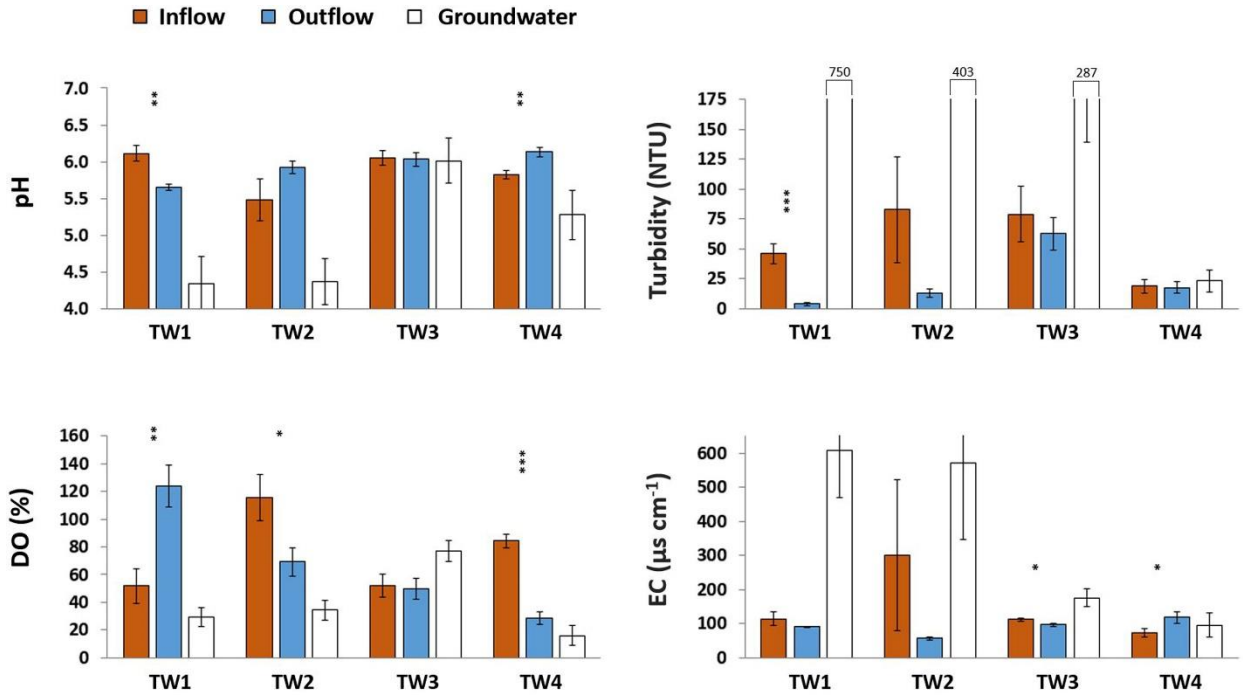

Figure 2. Differences between the inflow (red), outflow (blue), and the groundwater (white) physicochemical characteristics; pH, Turbidity, DO, and EC.

The error bar shows the standard error for each column. Significant differences between the inflow and outflow are shown as: * $p < 0.05$, ** $p < 0.01$, *** $p < 0.001$.

288

289 The outflow concentrations of NO_3^--N was lower than the inflow for TW2, TW3, and

290 TW4 wetlands, although the difference was significant only for TW2 (U =9, Z = -3.682, $p <$

291 0.001) (Fig. 3). In contrast, for TW1, NO_3^--N outflow concentrations were significantly

292 higher than the inflow (t (20) = -5.34, $p < 0.001$). In general, the reduction of NO_3^--N

293 between outflow and inflow was significantly higher when the pH of the wetland water was

294 high, and EC was low (r_s = 0.36, $p < 0.02$; r_s = -0.34, $p < 0.05$).

295 The outflow concentration of NH_4^+-N was lower than the inflow for TW1, TW2 and

296 TW3 wetlands, although the difference was significant only for TW1 and TW2 (U = 7.5, Z =

297 -3.58, $p < 0.001$; $U = 0$, $Z = -4.32$, $p < 0.001$). For example, for TW2, the concentrations of
298 NH_4^+-N decreased by over 0.4 mg L^{-1} in the first three sampling events (Fig. 3). The
299 difference between the concentrations of NH_4^+-N in the outflow and inflow was significantly
300 affected by rainfall, where the rise in 3-day antecedent rainfall decreased NH_4^+-N reduction
301 rates of the sites ($r_s = -0.38$, $p < 0.01$). Additionally, the reduction of NH_4^+-N increased at
302 high DO and low EC ($r_s = 0.5$, $p < 0.001$; $r_s = -0.61$, $p < 0.001$). A multiple linear regression
303 model showed that the parameters with the highest explanatory power for NH_4^+-N reduction
304 were pH and EC, where the change in concentration between inflow and outflow is given by:

$$\Delta NH4 = 0.167 \times (pH) - 0.002 \times (EC) - 0.753 \quad (11)$$

($F_{(2,30)} = 5.26$, $p = 0.01$, $R^2 = 0.26$)

305 The reduction of DON, TP and TSS concentrations in the outflow were positively
306 autocorrelated ($r_s > 0.46$, $p < 0.01$), and reduction of DON and TP were high when NO_3^--N
307 reduction was low ($r_s < -0.39$, $p < 0.01$). Sites TW2 and TW4, which were very efficient at
308 reducing the outflow of NO_3^--N, had low rates of DON, TP and TSS reduction (Fig. 4). In
309 TW4, the concentrations of DON, TP and TSS were even higher in the outflow compared to
310 the inflow (DON: $U = 9$, $Z = -3.38$, $p < 0.001$; TP: $U = 3$, $Z = -3.80$, $p < 0.001$, Fig. 4).
311 Conversely, TW1 had very little NO_3^--N reduction, but had significant reductions in DON,
312 TP and TSS concentrations at 0.44 ± 0.06, 0.26 ± 0.02 and 31.6 ± 11.7 mg L^{-1}, respectively
313 ($U = 6$, $Z = -3.83$, $p < 0.001$; $U = 0$, $Z = -3.98$, $p < 0.001$ and $U = 10$, $Z = -3.32$, $p < 0.001$).
314 Reduction of DON, TP and TSS across the sites was positively correlated with DO and
315 negatively with pH (DO: $r_s > 0.42$, $p < 0.01$; pH: $r_s < -0.30$, $p < 0.05$). The reduction rates of
316 both TP and TSS decreased at high turbidity ($r_s = -0.31$, $p < 0.05$; $r_s < -0.30$, $p < 0.05$).
317 Overall, a multiple linear regression model using stepwise method showed DO, pH, ORP and
318 EC as the main predictors of DON reduction, and for TP reduction the main predictors were
319 DO and pH (Eq. 12 and 13).

$$\log(\Delta\mathrm{DON} + 0.4) \quad (12)$$

$$= 0.447 \times (\log(\Delta\mathrm{DO} + 5)) - 0.416 \times (pH) - 0.001 \times (ORP) + 0.002 \times (ELC) + 0.447$$

($F_{(4,26)}$ = 11.94, p < 0.001, R^2 = 0.59)

320

$$\Delta TP = 0.196 \times (\log(\Delta\mathrm{DO} + 5)) - 0.18 \times (pH) + 0.751 \quad (13)$$

($F_{(2,30)}$ = 9.56, p < 0.001, R^2 = 0.35)

321

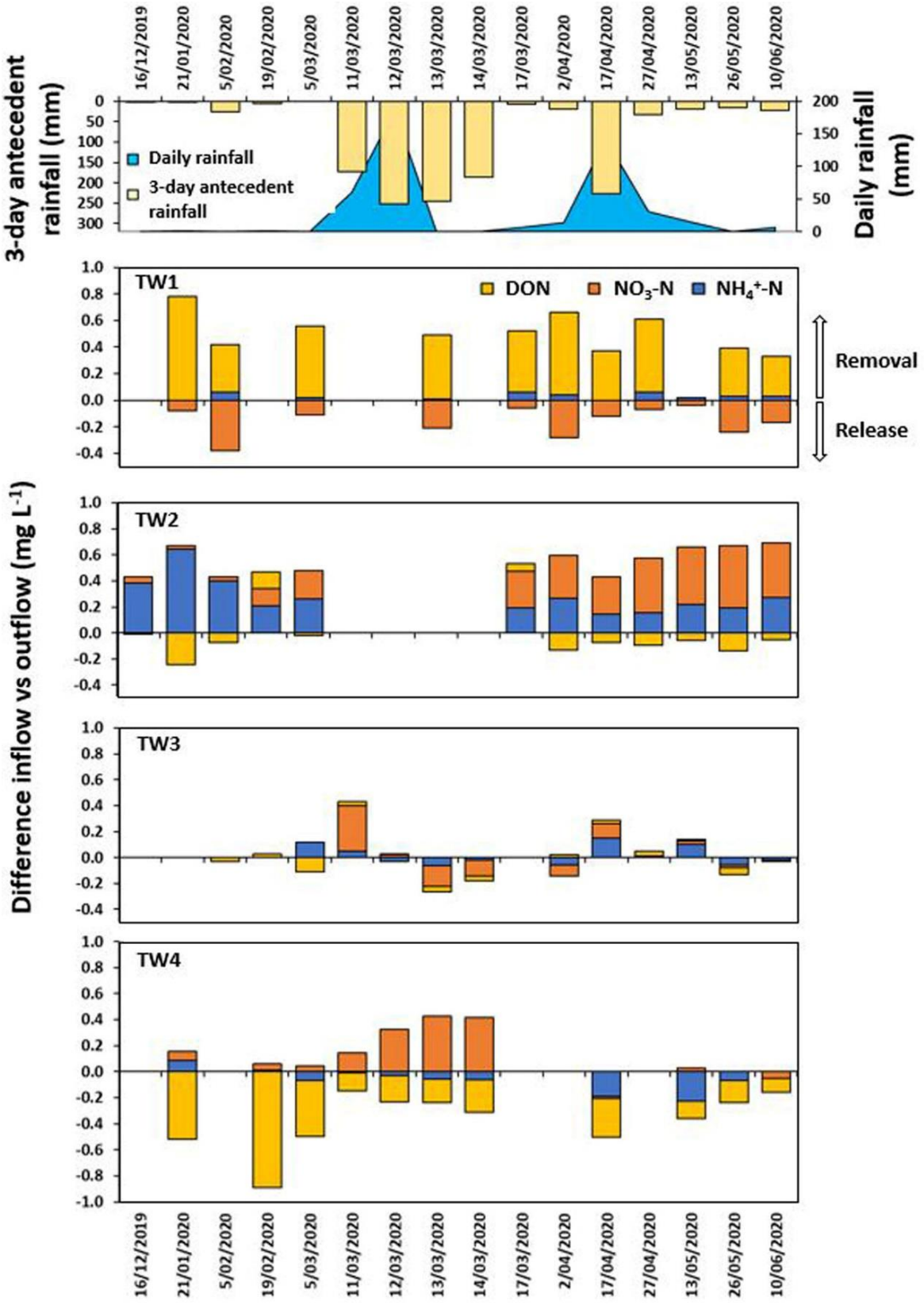

Figure 3. Daily and 3-day antecedent rainfall (mm) and changes in nitrogen concentrations (DON, NO_3^--N, NH_4^+-N) for four wetland treatment systems in tropical Australia. Positive values are removals, and negative values are release.

322

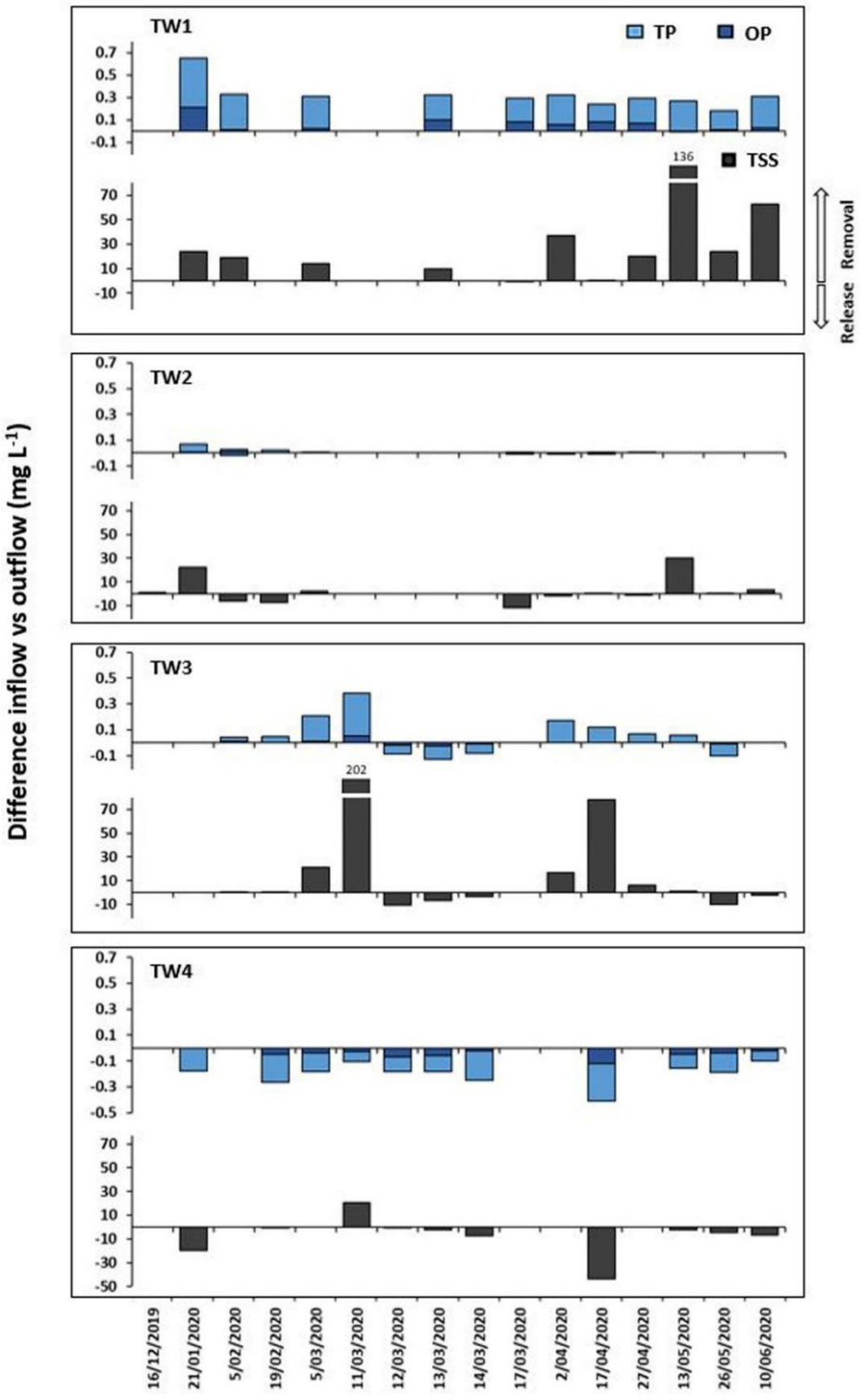

Figure 4. Daily and 3-day antecedent rainfall (mm) and changes in total suspended solids (TSS) and phosphorus concentrations (TP and OP) for four wetland treatment systems in tropical Australia.

Positive values are removals, and negative values are release.

3.4 Modelling performance of constructed wetlands

The results of the steady-state and event-based models for the TW3 site showed much higher cumulative removal of NO_3^--N and NH_4^+-N when the site is vegetated in comparison to the non-vegetated scenario (Fig. 5 and 6). Decreased NO_3^--N and NH_4^+-N removal in the un-vegetated state is a direct consequence of the model assumptions, namely denitrification and plant uptake was set to zero in the non-vegetated case. Although denitrification can occur in the absence of vegetation, such as in environments with low oxygen, high carbon, and high NO_3^--N concentrations (Seitzinger, 1988; Veraart et al., 2011), on-site denitrification in TW3 was not detected. Without denitrification and plant uptake, NO_3^--N removal is episodic and dominated by the inflow-outflow relationships, with net generation modelled under certain conditions. Under both vegetated and non-vegetated conditions, the model simulates net generation of NH_4^+-N and transformation of NH_4^+-N to NO_3^--N. In contrast, PON removal is assumed to have no explicit dependence on vegetation coverage in the model, which results in minimal differences in cumulative PON removal between the vegetated and non-vegetated states (Fig. 5). PON removal is dominated by settling throughout the event.

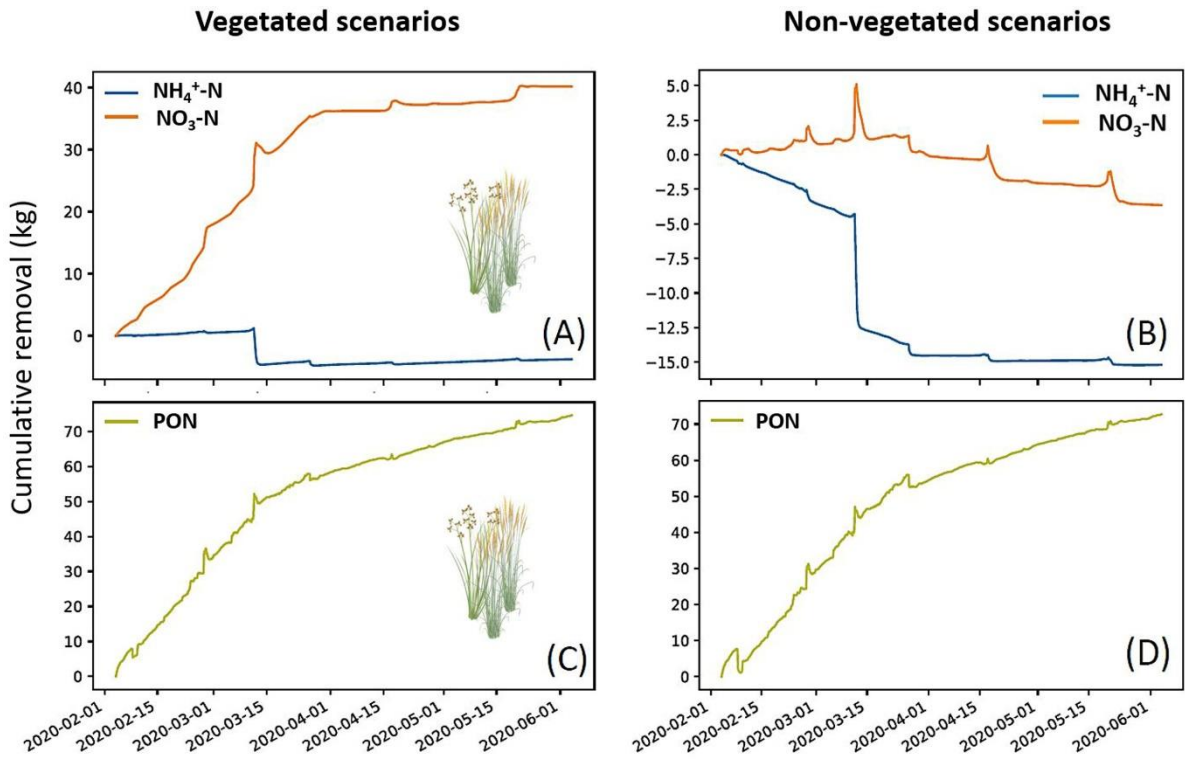

Figure 5. Cumulative removal (kg) of NH_4^+-N, NO_3^--N (A, B) and PON (C, D) modelled for TW3 in the event-based model across 121-days with (A, C) and without vegetation (B, D).

Positive values are removals, and negative values are release.

338

339 The results of the steady-state model for site TW3 showed that both NO_3^--N and
340 NH_4^+-N concentrations and the inflow rate affected the performance of the wetland in
341 removing NO_3^--N and NH_4^+-N, with vegetation coverage enhancing these differences (Fig.
342 6). As with the event-based model, the vegetated scenario showed the highest removal of
343 NO_3^--N and NH_4^+-N compared to the non-vegetated case for all scenarios. In the non-
344 vegetated case, NH_4^+-N reduction is only expected under low flow-high concentration
345 scenarios, with low and medium concentrations corresponding to release. As the inflow rates
346 increase, all concentration scenarios tend to a no-removal state. In comparison, NO_3^--N
347 removal is only observed during low flow-medium concentration events for the non-
348 vegetated case, with low or high concentrations corresponding to release.

In contrast, the vegetated case sees NO_3^--N and NH_4^+-N removal for most scenarios, with only low flow-low concentration scenarios leading to slight NH_4^+-N release. The release at low flow-low concentration is likely due to the lower nitrification rate driven by the low NH_4^+-N concentrations and NH_4^+-N sediment release. NO_3^--N proportional removal is greatest at high concentration and lowest at low concentration across all inflows, and as with NH_4^+-N p has a roportional removal decline with increasing inflow. Lower inflows correspond to lower mass influxes and higher residence times, providing a greater opportunity for nitrifying, denitrifying, and anammox bacteria to process the NO_3^--N and NH_4^+-N.

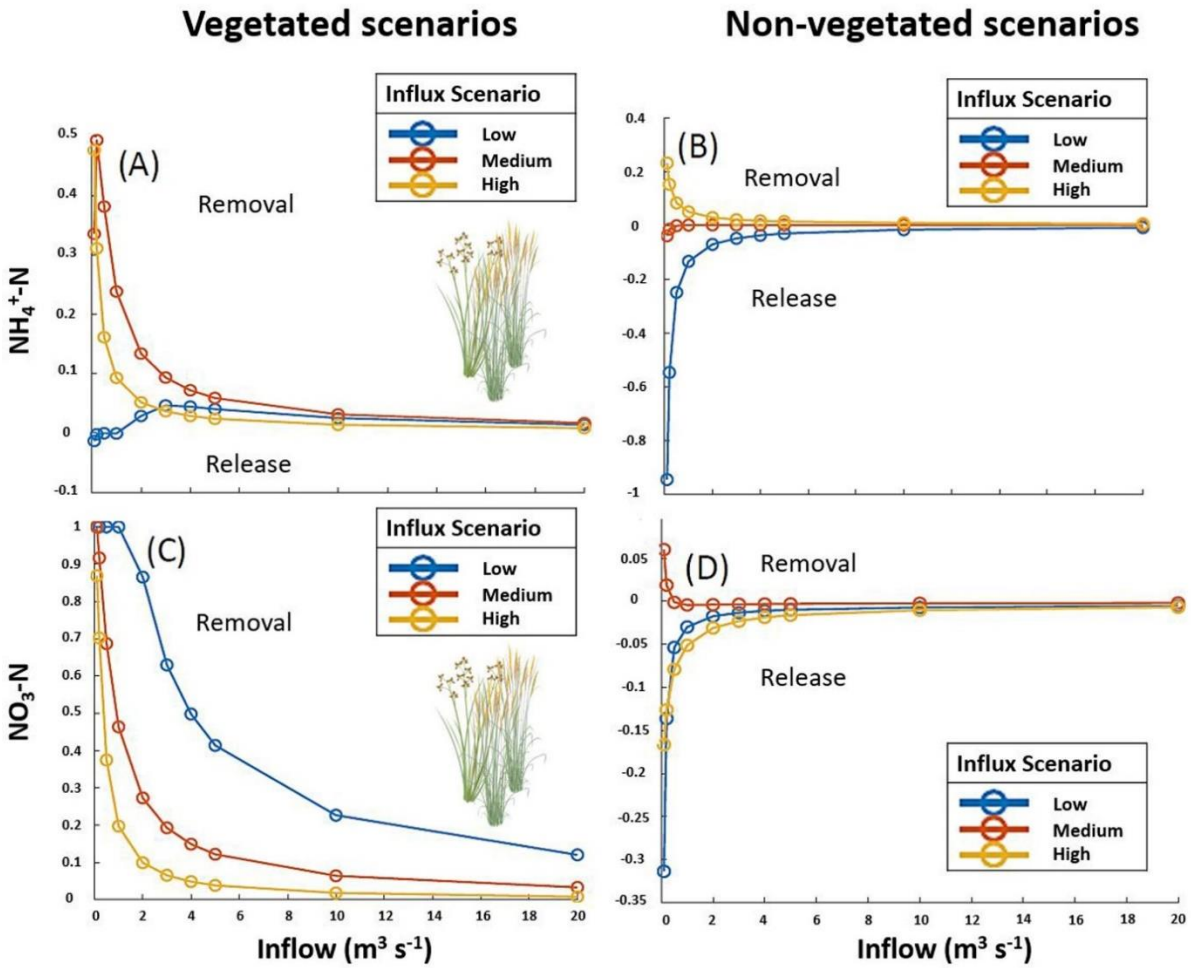

Figure 6: Proportion of inflow nitrogen load (for NH_4^+-N and NO_3^--N) removed under vegetated (A, C) and non-vegetated (B, D) scenarios for TW3 under different inflow conditions (1-20 m^3 s^{-1}) and different influx scenarios, modelled using the steady-state assumptions.

Proportions above zero mean removal and below zero mean release. Concentrations for low, medium and high scenarios are as per Table S2.

361

362 4. Discussion

363 The treatment wetlands varied in their characteristics; TW2, TW3, and TW4 had the potential
364 for denitrification at the time of sampling, but only TW2 and TW4 consistently removed
365 NO_3^--N, and TW2 removed both, NO_3^--N and NH_4^+-N throughout all the sampling period.

366 Low-oxygen conditions in soil with high C, low bulk density, and water with high NO_3^--N
367 concentrations promoted denitrification and NO_3^--N removal in these sites (Kulkarni et al.,
368 2008; Zhou et al., 2014; Ray et al., 2019). Removal of NH_4^+-N in TW2 could result from
369 macrophyte consumption, and the occasional release of NH_4^+-N in TW4 could be caused by
370 organic matter remineralisation. Both sites consistently exported DON and had lower DO
371 concentrations and higher pH in the outflow than the inflow, suggesting high primary
372 production and high soil respiration.

373 Comparatively, TW1 and TW3 did not remove nitrogen at the time of sampling but
374 acted as a sedimentation basin removing TP and TSS from the receiving water. In TW1, no
375 denitrification could be detected nor nitrogen uptake, probably due to the oxic conditions of
376 the soil of this recently constructed wetland and the lack of an established microbial
377 community (Duncan and Groffman, 1994). The developing microbial community could be
378 consuming DON, and nitrification (conversion of NH_4^+-N to NO_3^--N) would be the dominant
379 process at this site where water gets highly oxidised as it flows through the treatment
380 systems. Acidic soils (pH < 5.0) also may have limited the denitrification potential of TW1
381 (Jalota et al., 2018). This site was the only one with consistently higher NO_3^--N
382 concentrations in the outflow compared to the inflow. This could be either a result of the
383 sampling design because there is a groundwater spring in the middle of the wetland or due to
384 land-use legacy, reflecting flushing of nitrogen from soils with a history of fertilisers (Brush,
385 2009).

386 Site TW3 had low-oxygen conditions in the soil, which promoted denitrification
387 during the experiment (where NO_3^--N was added), but in the field, most nitrogen was in the
388 form of NH_4^+-N. The high NH_4^+-N concentrations could be due to low soil ORP that
389 prevented nitrification and favoured DNRA (dissimilatory nitrate reduction to ammonia
390 (Silver et al., 2001). Site TW3 showed occasional nutrient removal capacity, probably due to

increased vegetation cover and the establishment of a soil microbial community as the wetland matured (Kadlec and Wallace, 2008).

4.1 Management and implications

The analyses of the inflow versus outflow water quality parameters suggest different nutrient pathways for the wetlands treatment systems. These pathways appear associated with time since construction, nutrient loads, vegetation and soil microbial establishment, soil and water characteristics of the wetland, and land-use history (Brush, 2009). Overall, all treatment wetlands provide some form of improvements to water quality. However, the net loss of nitrogen can only occur by removing NO_3^--N through denitrification (Kulkarni et al., 2008), so the management of these wetlands should be targeted for this process to occur.

Figure 7 presents a schematic diagram providing a plausible explanation for the differences in the treatment wetlands performance and the conditions that need to be targeted for improved denitrification. During the early stages of construction (Panel A), or in sites where soil conditions are poor, microbial communities will dominate nitrogen fluxes (Mushinski et al., 2019). In these conditions, DO in the water could be high, and the wetland will function as a sediment trap, decreasing TSS and TP from the water column. In these conditions, DON could be consumed by the developing soil microbial community (Kadlec and Wallace, 2008). As the microbial community establishes and vegetation starts to grow (Panel B), carbon content will increase in the soil, and microbial respiration will consume DO (Kulkarni et al., 2008). As a result of increased drag from the vegetation, water flows are also likely to decrease, resulting in lower DO (Nakamura and Stefan, 1994). In these conditions, nitrification-denitrification is favoured, and NO_3^--N is removed, NH_4^+-N could be either removed by the plants or exported if water stagnation is persistent, and DON could be either

consumed by the microbial community or exported due to increased primary productivity (Liao et al., 2019). Higher productivity will also result in increased pH in the water column as CO_2 is consumed (Kadlec and Wallace, 2008).

Finally, if vegetation cover is excessive and water becomes stagnant (Panel C), the wetland becomes anaerobic, with very low or no DO (Nakamura and Stefan, 1994). These conditions will limit nitrification, and the low availability of NO_3^--N will limit denitrification. This could result in potentially high DON and NH_4^+-N exports, the latter potentially hazardous for aquatic animals, mainly if high pH generates high levels of NH_3 (Nugroho et al., 2007). These conditions could also increase greenhouse gas emissions as the expected by-product (CH_4 and N_2O) (Kavehei et al., 2021). Overall, management of constructed wetlands should aim at maintaining conditions as in Panel B.

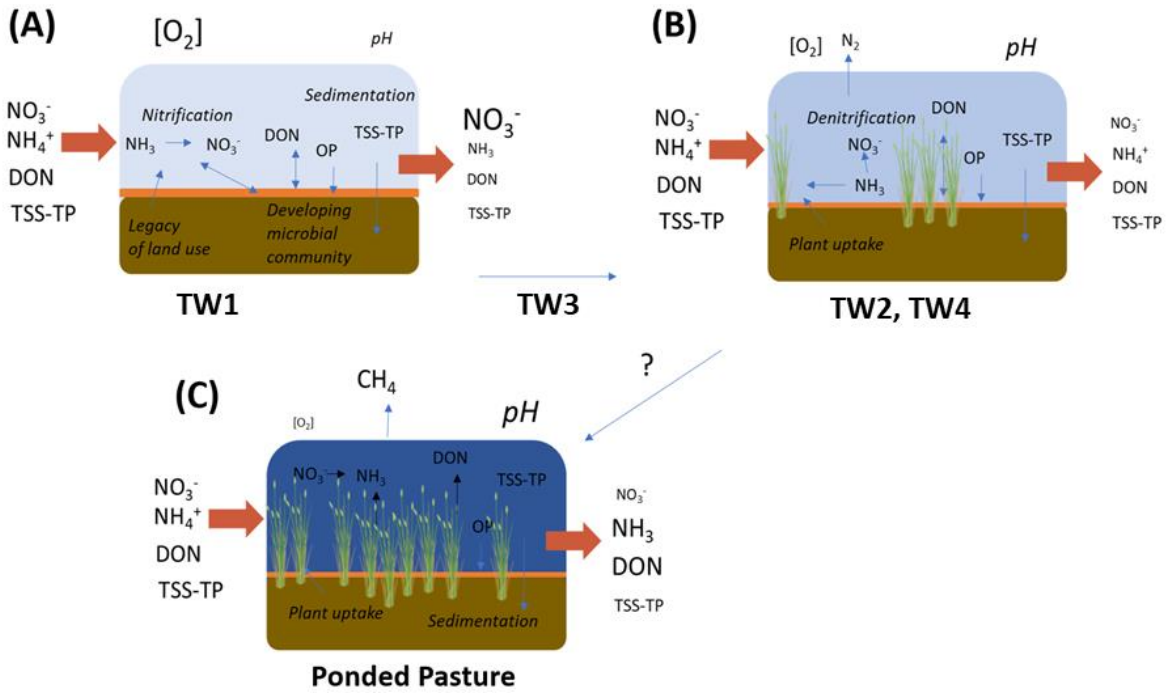

Figure 7. A schematic diagram, providing a plausible explanation for the differences in performance of the treatment wetlands. Relative changes in the concentrations between the inflows and outflows are indicated by the relative text sizes, increasing text sizes indicating enrichment and decreasing text sizes showing uptake or losses.

We have identified conditions that could favour denitrification and thus NO_3^--N removal in the treatment systems. Soil pH has a well-known impact on coupled nitrification-denitrification (Nugroho et al., 2007), with increased denitrification at pH values between 6 and 8 (Jalota et al., 2018). During the sampling, higher pH of outflow was associated with lower NO_3^--N concentrations in the outflow. Lower pH, along with low EC was also associated with reduced NH_4^+-N. Thus, water pH, along with EC, ORP, soil C and vegetation cover, could be good indicators of the performance of treatment wetlands for the removal of removing inorganic nitrogen in these tropical catchments.

5. Conclusion

All the treatment wetlands provided some form of improvements to water quality through different nutrient pathways associated with the time since construction, vegetation, and soil microbial establishment. The treatment wetlands can be designed and managed to enhance the environmental conditions for different pathways of nutrient removal. It is expected that as they mature and the vegetation cover increases, they will become important assets for nitrogen removal in the tropical agricultural landscape to enhance nutrient removal and protect sensitive receiving marine environments. Further research is recommended to investigate the capacity of treatment wetlands, from the establishment to maturity, to enhance nutrient removal and protect sensitive receiving water environments.

Acknowledgements

We want to thank all the farmers that provided access to their land and shared with us their local knowledge. MFA was supported by an Advance Queensland Industry Engagement Fellowship by the Queensland Government, Australia.

References

Adame, M.F., Franklin, H., Waltham, N., Rodriguez, S., Kavehei, E., Turschwell, M., Balcombe, S., Kaniewska, P., Burford, M., Ronan, M., 2019a. Nitrogen removal by tropical floodplain wetlands through denitrification. Marine and Freshwater Research 70, 1513-1521.

Adame, M.F., Hamilton, D.P., Roberts, M.E., Reis, V., Lu, J., Griffiths, M., Curwen, G., Ronan, M., 2019b. Tropical coastal wetlands ameliorate nitrogen export during floods. Frontiers in Marine Science 6, 671.

Adame, M.F., Pettit, N.E., Valdez, D., Ward, D., Burford, M.A., Bunn, S.E., 2017. The contribution of epiphyton to the primary production of tropical floodplain wetlands. Biotropica 49, 461-471.

Almasri, M.N., Kaluarachchi, J.J., 2004. Assessment and management of long-term nitrate pollution of ground water in agriculture-dominated watersheds. Journal of Hydrology 295, 225-245.

Brush, G.S., 2009. Historical land use, nitrogen, and coastal eutrophication: A paleoecological perspective. Estuaries and Coasts 32, 18-28.

Davis, A.M., Pearson, R.G., Brodie, J.E., Butler, B., 2017. Review and conceptual models of agricultural impacts and water quality in waterways of the Great Barrier Reef catchment area. Marine and Freshwater Research 68, 1-19.

Duncan, C.P., Groffman, P.M., 1994. Comparing microbial parameters in natural and constructed wetlands. Journal of Environmental Quality 23, 298-305.

Galloway, J.N., Aber, J.D., Erisman, J.W., Seitzinger, S.P., Howarth, R.W., Cowling, E.B., Cosby, B.J., 2003. The nitrogen cascade. Bioscience 53, 341-356.

471 Galloway, J.N., Cowling, E.B., 2002. Reactive nitrogen and the world: 200 years of change.
472 AMBIO: A Journal of the Human Environment 31, 64-71.

473 Hansen, A.T., Dolph, C.L., Foufoula-Georgiou, E., Finlay, J.C., 2018. Contribution of
474 wetlands to nitrate removal at the watershed scale. Nature Geoscience 11, 127-132.

475 Haritash, A.K., Dutta, S., Sharma, A., 2017. Phosphate uptake and translocation in a tropical
476 Canna-based constructed wetland. Ecological Processes 6, 1-7.

477 Jalota, S., Vashisht, B., Sharma, S., Kaur, S., 2018. Understanding Climate Change Impacts
478 on Crop Productivity and Water Balance. Academic Press.

479 Jones, H.P., Hole, D.G., Zavaleta, E.S., 2012. Harnessing nature to help people adapt to
480 climate change. Nature Climate Change 2, 504-509.

481 Kadlec, R.H., Wallace, S., 2008. Treatment wetlands 2nd edition. CRC press, Boca Raton,
482 Florida, USA.

483 Kavehei, E., Iram, N., Rashti, M.R., Jenkins, G.A., Lemckert, C., Adame, M.F., 2021.
484 Greenhouse gas emissions from stormwater bioretention basins. Ecological Engineering 159,
485 106120.

486 Kulkarni, M.V., Groffman, P.M., Yavitt, J.B., 2008. Solving the global nitrogen problem: it's
487 a gas! Frontiers in Ecology and the Environment 6, 199-206.

488 Land, M., Granéli, W., Grimvall, A., Hoffmann, C.C., Mitsch, W.J., Tonderski, K.S.,
489 Verhoeven, J.T., 2016. How effective are created or restored freshwater wetlands for nitrogen
490 and phosphorus removal? A systematic review. Environmental Evidence 5, 9.

491 Liao, K., Hu, H., Ma, S., Ren, H., 2019. Effect of microbial activity and microbial
492 community structure on the formation of dissolved organic nitrogen (DON) and bioavailable
493 DON driven by low temperatures. Water research 159, 397-405.

494 Mitsch, W.J., Gosselink, J.G., 2000. The value of wetlands: importance of scale and
495 landscape setting. Ecological economics 35, 25-33.

496 Mushinski, R.M., Phillips, R.P., Payne, Z.C., Abney, R.B., Jo, I., Fei, S., Pusede, S.E., White,
497 J.R., Rusch, D.B., Raff, J.D., 2019. Microbial mechanisms and ecosystem flux estimation for
498 aerobic NOy emissions from deciduous forest soils. Proceedings of the National Academy of
499 Sciences 116, 2138-2145.

500 Nakamura, Y., Stefan, H.G., 1994. Effect of flow velocity on sediment oxygen demand:
501 Theory. Journal of Environmental Engineering 120, 996-1016.

502 Nielsen, L.P., 1992. Denitrification in sediment determined from nitrogen isotope pairing.
503 FEMS Microbiology Letters 86, 357-362.

504 Nugroho, R.A., Röling, W., Laverman, A., Verhoef, H., 2007. Low nitrification rates in acid
505 Scots pine forest soils are due to pH-related factors. Microbial Ecology 53, 89-97.

506 Ray, S., Scholz, M., Haritash, A., 2019. Kinetics of carbon and nitrogen assimilation by
507 heterotrophic microorganisms during wastewater treatment. Environmental monitoring and
508 assessment 191, 1-11.

509 Robertson, E.K., Bartoli, M., Brüchert, V., Dalsgaard, T., Hall, P.O., Hellemann, D.,
510 Hietanen, S., Zilius, M., Conley, D.J., 2019. Application of the isotope pairing technique in
511 sediments: Use, challenges, and new directions. Limnology and Oceanography: Methods 17,
512 112-136.

513 Rousseau, D.P., Lesage, E., Story, A., Vanrolleghem, P.A., De Pauw, N., 2008. Constructed
514 wetlands for water reclamation. Desalination 218, 181-189.

515 Seitzinger, S.P., 1988. Denitrification in freshwater and coastal marine ecosystems:
516 ecological and geochemical significance. Limnology and oceanography 33, 702-724.

517 Steingruber, S.M., Friedrich, J., Gächter, R., Wehrli, B., 2001. Measurement of
518 denitrification in sediments with the 15N isotope pairing technique. Appl. Environ.
519 Microbiol. 67, 3771-3778.

520 Veraart, A.J., de Bruijne, W.J., de Klein, J.J., Peeters, E.T., Scheffer, M., 2011. Effects of
521 aquatic vegetation type on denitrification. Biogeochemistry 104, 267-274.

522 Wang, H., Gao, J.-e., Li, X.-h., Zhang, S.-l., Wang, H.-j., 2015. Nitrate accumulation and
523 leaching in surface and ground water based on simulated rainfall experiments. PLoS One 10,
524 e0136274.

525 Zhou, S., Borjigin, S., Riya, S., Terada, A., Hosomi, M., 2014. The relationship between
526 anammox and denitrification in the sediment of an inland river. Science of the total
527 environment 490, 1029-1036.

528